



www.ericjournal.ait.ac.th

Web-Based System Design to Monitor and Control the Mismatching Effects in a Vast Solar Farm

Ahmed J. Abid^{*1}, Adel A. Obed[#], and Fawzi M. Al-Naima⁺

Abstract – It is a known fact that mismatching in the PV array leads to a drastic reduction in the system efficiency. Soiling and partial shading are the main reasons for this mismatching. In vast solar PV farms, the detection of the mismatching in an individual PV panel is a difficult task since it is usually done manually. In this paper, a new design is proposed to monitor the production of individual PV panel periodically no matter how it is connected in the array. The proposed design allows the user to monitor the open circuit voltage (VOC), the short circuit current (ISC) and the delivered power for each PV panel in the farm. It is also capable of controlling each panel to work at its maximum power point (MPP) using a built in maximum power point tracking (MPPT) sub-circuit on each solar panel. The overall mismatching for each string will be calculated and presented online with a website which is designed for this purpose. The presented system depicts a complete wireless sensor network, which does not need any extra wiring and is characterized by being of low cost, reliable and efficient.

Keywords – fault detection, mismatching effect, MPPT, photovoltaic solar farms, WSN.

1. INTRODUCTION

The establishment of a productive PV solar farm needs a large open land area to install. This area could be on mountain slopes, floated on the lakes, or any odd land, but even with a flat land it needs a hard work for monitoring and controlling the performance of all these very large numbers of individual panels. Checking of each PV panel in the farm will be a major problem, especially in areas that are hardly affected by soiling. Soiling could affect only the panels in the solar farm or could affect some individual ones, but in both cases the power production capability will certainly be decreased [1]–[4] whether the PV panels are connected in series, in parallel, or in array [5], [6]. The dust constitute one of the major problems among all other soiling factors especially in the Middle East and North Africa [7]–[10]. Researchers in [11] proposed the use of the PV power-line with a transceiver to control and monitor the movement of a solar tracker, however this paper suggests a system for monitoring and controlling the faults for the fixed solar panels.

Wi-Fi network investment in managing and monitoring the power consumption for indoor usage was discussed briefly in [12], [13]. This paper will adopt a similar strategy for an outdoor vast network. It is also feasible to use the same network to adopt the algorithms presented in [14], [15] in case the solar panels use trackers and that may be accomplished easily since all

calculations are carried out in the main computer and the data of the tilt and elevation angles are sent using the adopted network.

In addition, the proposed system suggests the addition of a low cost electronic circuit attached to each solar panel (module). This circuit can control and measure the produced power in each panel, then broadcast the data via Wi-Fi to the main control and monitoring unit (MCMU). This MCMU consists of a computer and a dedicated HTML website designed for this purpose. The user can monitor wirelessly individual solar panels in the farm to have a complete view about the open circuit voltage V_{OC} , the short circuit current I_{SC} , and the produced power to be compared with the ideal values. It is also possible to disconnect any bad PV panels from the string or boost its voltage to match the other panels in the string. Additionally, the proposed system has its own built in MPPT circuit to keep each single solar panel at the MPP.

In addition, the system takes into consideration that all panels are identical when installed, so any mismatching may be caused by external effects. The research work in [16], [17] offered detecting system faults from monitoring the main load then using some algorithms to find the exact location of the faulty PV panels. However, this is different for the proposed system in this paper which can detect faults directly since it gathers all data directly from each solar module. Other researchers in [18] suggested an artificial neural network to detect the faults caused by partial shading only. The use of ZigBee as a transceiver with Arduino Mega was suggested in [19], but such design has many disadvantages such as being of a large size of the Arduino Mega compared to the NodeMCU, costing around 40 USD only for ZigBee, and requiring a special receiver to read the ZigBee signal.

The main objectives of the present investigation are:

1. To detect the electrical and mechanical faults in the large PV farm.

^{*}Technical Instructors Training Institute, Middle Technical University, Baghdad, Iraq.

[#]Electrical Engineering Technical College, Middle Technical University, Baghdad, Iraq.

⁺Department of Computer Engineering, Al-Mamoon University College, Baghdad, Iraq.

¹Corresponding author:

Tel: + 9647706577624.

E-mail: dr.ahmedjabbar@mtu.edu.iq.

2. To monitor the performance of each single PV panel in the array.
3. To control the fault and to decrease the consumed time and money to find it.
4. To reduce the mismatching effects in the large PV array.
5. To track the MPP on the PV panel scale.
6. To localize the soiling spots in the PV array.

The remaining parts of this paper are organized as follows. Section 2 presents the soiling accumulation, section 3 describes the mismatching effects, section 4 explains the system design, section 5 discusses the results and finally, section 6 concludes the article.

2. SOILING ACCUMULATION

The photovoltaic soiling index (PVS_I) is an indicator for the performance of PV panels under exposure to dust at the standard test conditions (STC) [20], [21]. Soiling is described as the dirt accumulation on the solar panel modules and is an important loss factor particularly in locations when there are very dry conditions, scarce rain, and even frequent dust or sand storms [22].

The characteristics of soiling accumulation on solar panels are affected by two independent parameters; the local environment and the dust properties such as the shape, constituents, weight and size [22]. These properties play important role in dust scattering and lead to some different problems that cause a soil accumulation on solar panels. Below is a list of some of these factors and types which may affect each other as described by [23]–[27]:

- *Environment factors*: irradiation, wind movement, wind direction, dust storm, temperature [28], air pollution, air pressure, volcano and snow.
- *Dust type*: carbon, soil and sand, clay, bacteria.
- *Location and insulation*: sandy area, industrial area, latitude and longitude, glass material, orientation, height, tilt angle and flat surface.

There are many dust-accumulation mitigation strategies discussed by researchers such as [29], but dust-accumulation is still one of the major problems affecting the efficiency of the vast solar farms.

3. MISMATCHING EFFECTS

The mismatching in solar modules or solar cells may be due to many factors, one of them is the use of non-identical solar modules or solar cells. Every type of PV module has a variable specification caused by processing characteristics. Even the response to the variation of the solar irradiation may be different, since it depends on the manufacturer characteristics and material like the reflection of the protection glass, heat dissipation of the panel, rated voltage and current [30]. For these reasons it is recommended to use the same type of the PV panel in the solar array. Another

important factor causing the mismatch losses in PV modules and arrays is the partial shading of the solar array because the solar cell with the lowest output will control the output of the entire PV module. This article assumes that all the PV panels are identical and there is no row-to-row collector shading. Hence, if any mismatching occurs it will be due to partial shading, soiling, or a fault in the wiring connections. Many articles discussed methods to reduce this effect. The configurations for parallel string with different length was discussed in [31]. A holistic review of mismatch loss was discussed by [32] from the manufacturing point of view. The work presented in [33] reviewed the most effective electrical and mechanical faults at the PV field, the researchers also gave a recommendation for future directions to implement a low-cost integrated circuit for real time applications. A single-phase grid inverter with buck-boost convertor to extract the maximum power simultaneously from two mismatched strings was presented in [34]. A reconfiguration technique was presented in [35] to find the optimal PV configuration for reducing the mismatch power losses.

4. SYSTEM DESIGN

In general, the suggested system consists of master and slave controllers. The master controller is software designed for this purpose while the slave controller consists of both software and hardware parts. Figure 1 shows the system modules but as a communication topology, the solar panels can be connected according to power requirement (in series, in parallel, or combined).

These controllers are connected via Wi-Fi network with a star topology. Star topology is a topology for a local area network (LAN) in which all nodes are individually connected to a central connection point, like a hub or a switch. However, there are more topologies that can be adopted in case of the slave controller is out of the master's coverage area.

In this design, a main computer, or smart phone will do the master controlling duties. Static internet protocol (IP) will be given for each PV panel. The master controller sends a request to individual slave controller to read the supplied power, ISC, and VOC, so the user can figure out if there is any solar panel or string of panels being shaded or partially shaded [36] or dusty [37], [38]. The master controller is also authorized to illuminate the bad panel or boost the voltage to match the MPPT for the panel.

4.1 Master Controller

The master controller software can be installed on any personal computer, laptop, or even a smart phone. It communicates with the slave controllers via wifi to gather and control the data. Figure 2 shows the designed website that displays the following information:

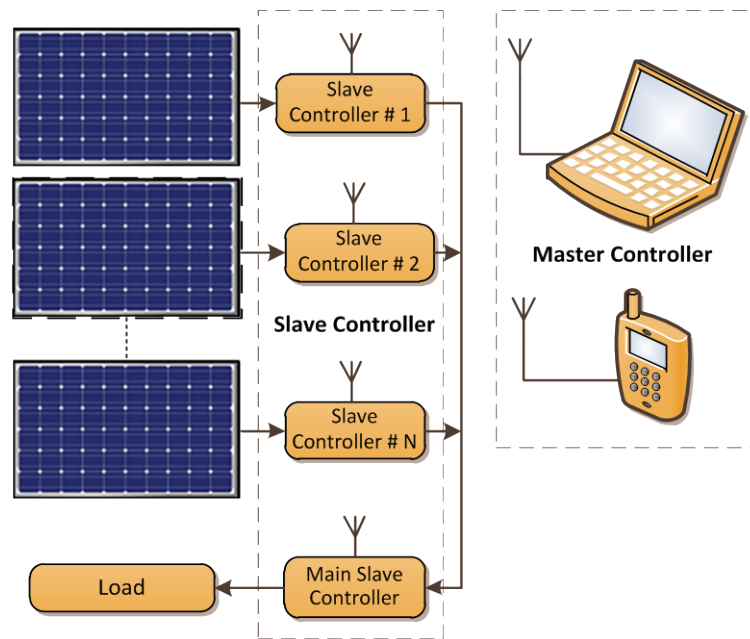


Fig. 1. System module.

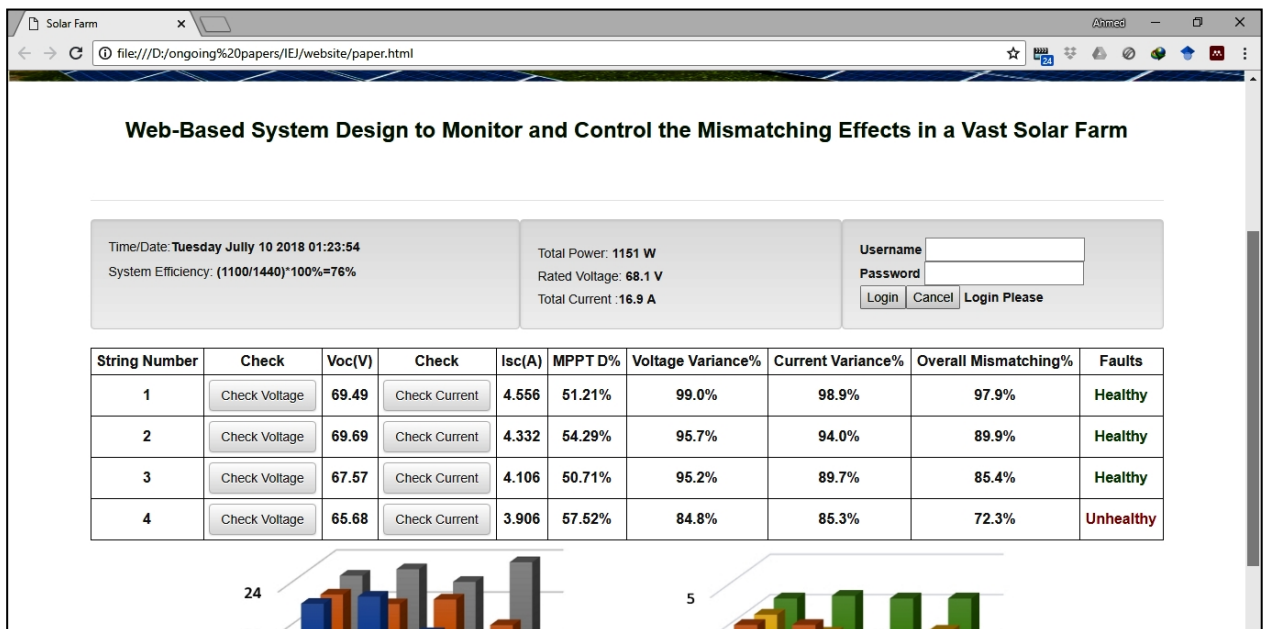


Fig. 2. Server website.

- **Power parameters:** total power, rated voltage, total current, the V_{OC} and I_{SC} for each PV panel, PV panel condition (by comparing the measured voltage and current with manufactured values), button to test the V_{OC} and I_{SC} (since the system does that periodically).
- **Time stamping:** time and date are used by the website to save the data with a time stamp to generate an evaluation report.
- **Authentication:** the website requests the login data (user name and password) before allowing the user to control the system.
- **Controlling data:** these data are important to understand the PV array behaviors which include the duty cycle of the MPPT, voltage and current variance for each string, overall mismatching, and the strings' condition.

The system adopts many software languages, as depicted in Figure 3, to design the website for establishing connections with the slaves to support the slave controller.

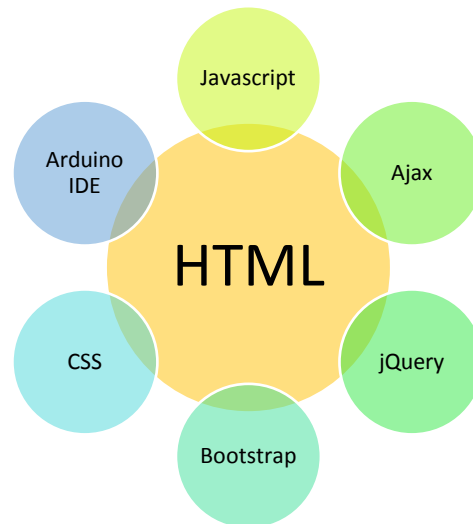


Fig. 3. The adopted software.

4.2 Slave Controller

The slave controller is mainly responsible to do all the measurements, control the output power to match the MPPT, disconnect the PV panel if necessary. It can control a single panel or its entire string and consist of the following two main parts:

- A. The software part includes the programming of NodeMCU using Arduino IDE software. NodeMCU has a built in Wi-Fi module and it is programmed to be a slave that receives requests from the master controller. The flowchart of Figure 4 shows how the slave controller reads voltage and current periodically and replays these to the master. In case the master requests the V_{OC} and I_{SC} the server slave will disconnect the PV Model from the string to calculate the V_{OC} and apply a short circuit to measure I_{SC} .
- B. The hardware electronic circuit is displayed in Figure 5, which consists of the following four sub-circuits.

(i) Current Sensing and Control

This sub circuit consists of a Power MOSFET (IRLZ44N) as switch which is responsible for shorting the circuit of the PV panel to measure the I_{SC} . The used current sensor is fully integrated, hall effect-based linear current sensor IC. The design adopts ACS712ELCTR-30A-T which has a sensitivity equal to 66mV/A. This sensor is supplied from the main bus bar via a voltage regulator (7805) so when the PV panel voltage is equal to zero, it will keep running and this is accomplished by synchronizing the Q2 to cut the solar panel from the string. The Zener diode D2 and R6 have been added to protect the Power MOSFET from the high voltage since this type can handle maximum gate-source voltage V_{GS} of $\pm 16V$.

(ii) Voltage Sensing and Control

This sub circuit is responsible for measuring the output voltage of the solar panel with or without

load. Normally the circuit reads the load voltage (Rated Voltage), but when the Q2 Power MOSFET is disconnected then the reading corresponds to the V_{OC} . The Q2 gate is protected as for Q1 using the Zener diode. To keep the string live Q3 is being turned on to illuminate the tested panel. The voltage divider which consists of R1 and R2 is responsible for scaling the voltage down since the ESP8266 ADC can handle maximum voltage of 5V. LED D1 gives an indication that the system is powered.

(iii) Maximum Power Point Tracker

The sub-circuit for the MPPT is responsible for tracking the MPP. The solar panels exhibit nonlinear relationship between the current and voltage characteristics which will produce a maximum power at only one particular operating point. Many researchers discussed this matter in detail like [39]–[41]. In this paper, we contemplate employing a separate MPPT sub-circuit for every single panel. This circuit is linked as part of the system circuitry. Its function is to keep the system at MPP and measure the bus bar voltage to match the produced voltage by this particular panel with bus the bar voltage. This MPPT has a great effect when the panel is connected in parallel, but since the panels are normally connected in series within the string, it will reduce the mismatching effect of the string on the array. The used buck-boost convertor which consists of (Q2, Q3, D4, L1, and C6), is responsible for controlling the output voltage according to Equation 1. The master controller is responsible for driving these two MOSFETs with two PWM signals.

$$D = V_o / (V_o - V_i) \quad (1)$$

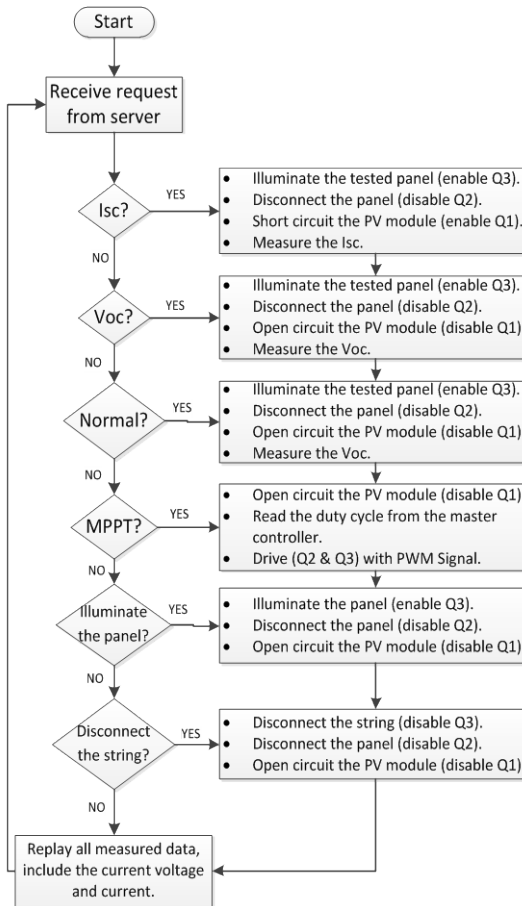


Fig. 4. Flowchart for the slave controller software.

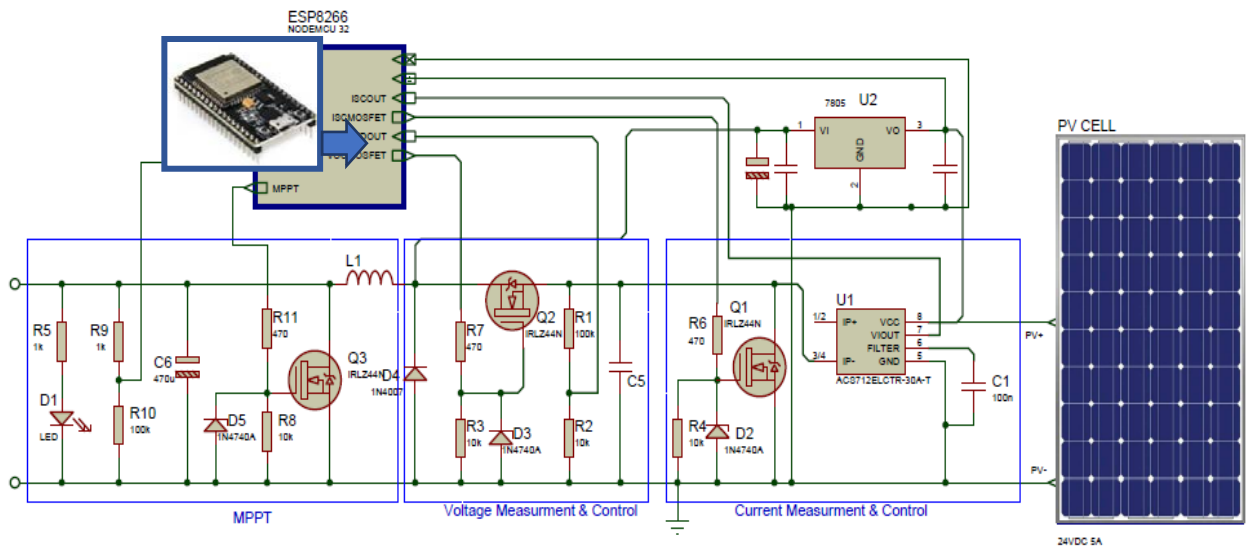


Fig. 5. System circuitry.

Table 1 shows a conclusion for the power MOSFET state of operations. It lists six different modes of operations.

(iv) *NodeMCU ESP-32S Board*

The main controller for this system is ESP8266-12 NodeMCU, which is considered as a slave. The main computer/controller will work as a master and collect data from the solar farm slaves. Only the master has the ability to request from the slaves to measure and evaluate the I_{SC} or V_{OC} for each solar

panel. This process is made once a day or periodically according to system setting to give the user a complete picture about each panel in the farm. A solar panel with low readings of I_{SC} or V_{OC} needs to be checked. In case all the panels are suffering from a low voltage, this gives an indication for cleaning the panel front glass from heavy dust. In case of soft shadow that is caused by tree branches or small clouds, these panels will be disconnected if the MPPT is failing to keep the states of voltage and current matching the other PV

panels in the farm. This MCU has a built in ADCs, Wi-Fi, and able to generate fast PWM signals, all

these capabilities and its small size make it very useful, cost efficient to be the slave controller.

Table 1. Power MOSFET state of operations.

Mode	State of operation	Q1	Q2	Q3
1	Measure ISC	ON	OFF	ON
2	Measure VOC	OFF	OFF	ON
3	Normal	OFF	ON	OFF
4	MPPT	OFF	PWM	PWM
5	Illuminate the panel	OFF	OFF	ON
6	Disconnect the string	OFF	OFF	OFF

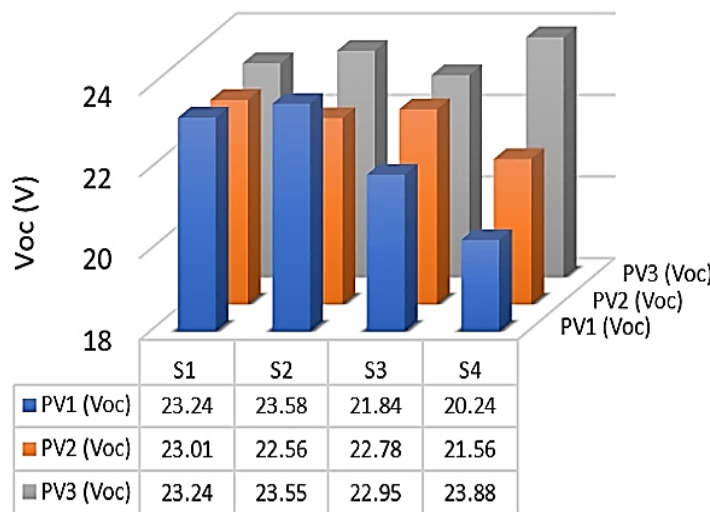


Fig. 6. Open circuit voltage test results.

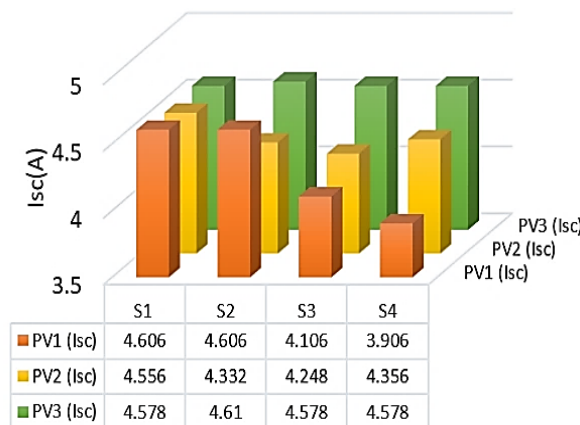


Fig. 7. Short circuit current test results.

5. RESULTS AND DISCUSSION

To validate the proposed system, an array of 12 identical PV modules is used with 4 strings in parallel, and with each string having three PV modules in series. The used PV module produces 24V DC, 5A (120 W), that means every string should produce 72V/5A, and the array has in total (72V/20A/1440W). The master controller is used to scan all the slave controllers to check the readings of the test results for the VOC and the ISC for each PV panel and display these data on the website as shown in Figures 6 and 7, respectively. These data are also saved

on an Excel file. The measured data are analysed by the master controller, and then displayed on the website.

Two voltages are measured by the same voltage sensor. It measures the normal voltage by default which is the accumulated voltage, in other word the PV1 voltage is measured, then PV2 voltage is equal to (PV1+PV2) and so on. The same sensor measures the VOC by disconnecting the panel from the string as mentioned before.

The string V_{OC} is calculated by two methods; the first is by disconnecting the string by that slave controller and measure the voltage, and the second, by

taking the algebraic sum of all the modules V_{OC} in the string, as depicted by Equation 2.

Unfortunately, the string I_{SC} is equal to the minimum I_{SC} in the string according to Equation 3, and this in effect causes a serious problem when the string is long because the fault in any panel in the string causes a dramatic reduction the produced power. This trade-off between reducing the current by using long string and the dramatic reduction of power caused by any partial shade, soiling, or fault, lead us to design such system that can localize the fault, and monitor every single panel in the array.

$$V_{OC}^{i_{string}} = \sum_{j=1}^n V_{OC}^j \tag{2}$$

$$I_{SC}^{i_{string}} = \min(I_{SC}^j) \tag{3}$$

Where i is the number of string, n is the PV module number in the string.

It follows that in Figure 2, we see that V_{OC} in string1 is equal to 69.49V *i.e.*, (23.24V+23.01V+23.24V), and the I_{SC} in string1 is equal to 4.602A, *i.e.*, min (4.648, 4.602, 4.648). To calculate the total produced power by the array, the mismatching effect must be taken into consideration. Hence, it is required to introduce the overall mismatching, which is the product of the voltage variance times the current variance. The string is considered healthy if the overall mismatch does not exceed 25%. The case study considers four strings with three modules, and the target here is to measure the overall mismatching in each string to detect any fault. To do this, it is required to calculate the voltage variance and current variance which are the most important factors for each string as follows:

$$\begin{aligned} \text{Overall mismatching} \\ &= \text{Voltage variance} \\ &\times \text{Current variance} \end{aligned} \tag{4}$$

$$\text{Voltage variance \%} = \left(\frac{V_{min}}{V_{max}} \right) * 100\% \tag{5}$$

$$\text{Current variance \%} = \left(\frac{I_{min}}{I_{max}} \right) * 100\% \tag{6}$$

Table 2 lists the measured data for the PV array which include V_{OC} , and I_{SC} for each PV module in the array, the voltage and current variance and the overall mismatching for each string. It also shows that string 4 has an overall mismatching <75%, which is considered as a shaded, or soiled string and needs be checked.

The faults in the PV system can be classified into the following two main types [42], [43]: the first type is an irreversible error which is caused by mechanical or

electrical problems, such as PV panel aging, open circuit, short circuits, and grounding. The second type is the temporary power loss faults that are caused by sheltering, such as cloud shadows. All these faults can be diagnosed from the given data according to following steps:

- (i) *Open Circuit*: this fault in the given connection affects the main supplied current, and any measured rate current gives a zero-ampere meaning there is such fault. Normally, all the modules in the same string will give zero amperes. But to localize this fault it is required to monitor the accumulated voltage inside the open circuit string and see when it is equal to zero.
- (ii) *Short Circuit*: this fault is easy to diagnose by reading the rated voltage. If it is equal to zero, it means there is a short circuit on the PV panel. Also, the rated measured current will be high since it means the I_{SC} and not rated current.
- (iii) *Mismatching*: this fault can be diagnosed from the mitigation in V_{OC} or I_{SC} between the strings. The mismatched string need to be scanned to localize the exact location of the fault, then reviewed to check if it is instantaneous or cumulative.
- (iv) *Grounding*: this fault causes a sudden high drop in the main voltage and current.
- (v) *Line-to-line fault*: this fault is caused by short circuit between the power lines from different string and can be detected by monitoring the string voltage.

This article offers a cost-efficient system and this can be clearly proved from its total cost. Table 3 shows a list of the quantities, estimated unit cost and total cost of the system slave controller only, since the master controller will entail no extra cost as it could be the PC, laptop, or a smart phone which is part of the existing system. A pictorial representation of the proposed circuit is small in size (10cm x 6cm) and can fit inside the solar panel in a plastic box and it is of a plug and play type as shown in Figure 8.

Finally, the system was implemented and underwent several tests like:

- Check the Wi-Fi connections between the master and the slave servers.
- Check the website functionality.
- Check the measurement accuracy.
- Measure the system response when the load is not matched the maximum power point parameters.

Most of these measurements were done with a set up made for this purpose as shown in Figure 9. This set up has a variable electronic load based on a power MOSFET with variable driven voltage. It slightly loads the PV array from zero to zero Watt, then calculates the voltage, current, and power at the maximum power point. It also calculates the V_{OC} , I_{SC} , and the fill factor. All the graphical representations are performed on MS Excel.

Table 2. Overall mismatching calculations.

	String ₁	String ₂	String ₃	String ₄
PV1 V _{OC} (V)	23.24	23.58	21.84	20.24
PV2 V _{OC} (V)	23.01	22.56	22.78	21.56
PV3 V _{OC} (V)	23.24	23.55	22.95	23.88
String Voltage (V)	69.49	69.69	67.57	65.68
V _{OC min} (V)	23.01	22.56	21.84	20.24
V _{OC max} (V)	23.24	23.58	22.95	23.88
Voltage variance %	99.0%	95.7%	95.2%	84.8%
PV1 I _{SC} (A)	4.606	4.606	4.106	3.906
PV2 I _{SC} (A)	4.556	4.332	4.248	4.356
PV3 I _{SC} (A)	4.578	4.61	4.578	4.578
I _{SC min} (A)	4.556	4.332	4.106	3.906
I _{SC max} (A)	4.606	4.61	4.578	4.578
Current variance %	98.9%	94.0%	89.7%	85.3%
Overall mismatching %	97.9%	89.9%	85.4%	72.3%

Table 3. Bill of quantities and the estimated cost.

Category	QTY	Refs	Value	Unit Cost (USD)	Total Cost (USD)
Capacitors	3	C1-C3	100nF	0.1	0.3
	3	C4-C6	470uF	0.2	0.2
	2	R1, R10	100kΩ	0.1	0.1
Resistors	4	R2-R4,R8	10kΩ	0.2	0.6
	2	R5, R9	1kΩ	0.3	0.3
	3	R6-R7, R11	470Ω	0.4	0.8
Integrated Circuits	1	U1	ACS712	3.95	3.95
	1	U2	7805	0.8	0.8
MSOFET with heatsink	3	Q1-Q3	IRLZ44N	1	3
	1	D1	LED	0.1	0.1
Diodes	2	D2-D3,D5	1N4740	1.15	2.3
	1	D4	1N4007	0.1	0.1
Inductor	1	L1		0.2	0.2
	1	J1		0.2	0.2
Connector	2	J3,J5		0.3	0.6
	1	J4		0.2	0.2
NodeMCU	1	ESP8266	32b	8.45	8.45
PCB Board	1	Two layers		5	5
Soldering Cost	1			5	5
Total Cost				*31.73 USD	

* Prices estimated based on reliable online marketing store on June 12, 2018.

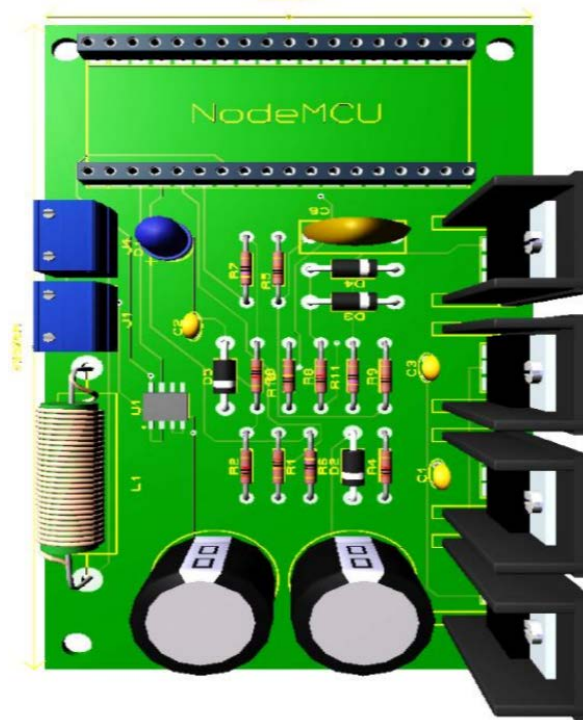


Fig. 8. A 3D module of the slave controller.



Fig. 9. The system under test.

6. CONCLUSION

In order to keep the running of a vast PV solar system reliable, safe and productive, it is envisaged to design and implement a system that detects faults automatically and classify them and this is in no doubt is a major challenge to the designer. The proposed system shows a fast and accurate fault detector. It can monitor the entire PV array in large solar farm wirelessly. The estimated cost (≈ 32 USD) is considered to be very low for such capabilities, and it is a step towards of the internet of PV

panel. Fault detection time decrease from hours into millisecond. The article does not only offer an MPPT on the PV panel level to reduce the mismatching effect, but also able to find and control the cause of the mismatching.

The offered system is cost efficient, reliable and is capable of locating and detecting major types of faults. It saves the time and cost in comparison with the traditional laborious manual methods and maximizes the produced power to match the load needs.

REFERENCES

- [1] Sulaiman S.A., Singh A.K., Mokhtar M.M.M., and Bou-Rabee M.A., 2014. Influence of dirt accumulation on performance of PV panels. in *Energy Procedia* 50: 50–56.
- [2] Rahman M.M., Islam M.A., Karim A.H.M.Z., and Ronee A.H., 2012. Effects of Natural Dust on the Performance of PV Panels in Bangladesh. *International Journal of Modern Education Computer Science* 4(10): 26–32.
- [3] Moharram K.A., Abd-Elhady M.S., Kandil H.A., and El-Sherif H., 2013. Influence of cleaning using water and surfactants on the performance of photovoltaic panels. *Energy Conversion and Management* 68: 266–272.
- [4] Sulaiman S.A., Mat M.N.H., Guangul F.M., and Bou-Rabee M.A., 2015. Real-time study on the effect of dust accumulation on performance of solar PV panels in Malaysia. In *Proceedings of 2015 International Conference on Electrical and Information Technologies, ICEIT 2015*, 25-27 March. Narrakech, Morocco, pp. 269–274.
- [5] Chamberlin C.E., Lehman P., Zoellick J., and Paultetto G., 1995. Effects of mismatch losses in photovoltaic arrays. *Solar Energy* 54(3): 165–171.
- [6] Wurster T.S. and M.B. Schubert 2014. Mismatch loss in photovoltaic systems. *Solar Energy* 105: 505–511.
- [7] Beattie N.S., Moir R.S., Chacko C., Buffoni G., Roberts S.H., and Pearsall N.M., 2012. Understanding the effects of sand and dust accumulation on photovoltaic modules. *Renewable Energy* 48: 448–452.
- [8] Said S.A.M., 1990. Effects of dust accumulation on performances of thermal and photovoltaic flat-plate collectors. *Applied Energy* 37(1): 73–84.
- [9] Cabanillas R.E. and H. Munguía. 2011. Dust accumulation effect on efficiency of Si photovoltaic modules. *Journal of Renewable and Sustainable Energy* 3(4).
- [10] Mekhilef S., Saidur R., and Kamalisarvestani M., 2012. Effect of dust, humidity and air velocity on efficiency of photovoltaic cells. *Renewable and Sustainable Energy Reviews* 16(5): 2920–2925.
- [11] Al-Naima F.M., Ali R.S., and Abid A.J., 2013. Solar tracking system: design based on GPS and astronomical equations. In *Proceedings of IT-DREPS Conference Exhibition, 29-31 May*, Amman, Jordan, pp. 1–6.
- [12] Abid A.J., 2017. Arduino based blind solar tracking controller. *An International Open Access Journal, IETI Trans. Comput.* 5(10): 24–29.
- [13] Al-Naima F., Ali R., and Abid A.J., 2014. Design of an embedded solar tracking system based on GPS and astronomical equations. *International Journal of Information Technology and Web Engineering* 9(1): 12–31.
- [14] Abid A.J. and A.H. Ali. 2017. Smart monitoring of the consumption of home electrical energy. *International Journal of Computer Trends and Technology* 47(2): 142–148.
- [15] Al-Naima F., Ali R.S., Abid A.J., Ghassemlooy Z., and Gao Z., 2013. A new power line communication modem design with applications to vast solar farm management. *Journal of Innovative Systems Design and Engineering* 4(14): 34–48.
- [16] Ji D., Zhang C., Lv M., Ma Y., and Guan N., Photovoltaic array fault detection by automatic reconfiguration. *Energies* 10(5): 699.
- [17] Chine W., Mellit A., Pavan A.M., and Lughi V., 2015. Fault diagnosis in photovoltaic arrays. In *Proceedings of 2015 International Conference on Clean Electrical Power (ICCEP)*, 16-18 June. Taormina, Italy, pp. 67–72.
- [18] Mekki H., Mellit A., and Salhi H., 2016. Artificial neural network-based modelling and fault detection of partial shaded photovoltaic modules. *Simulation Modelling Practice and Theory* 67: 1–13.
- [19] Al Dahoud A., Fezari M., Al-rawashdeh T.A., and Jannoud I., 2015. Improving monitoring and fault detection of solar panels using arduino mega in WSN. In *Proceedings of 17th International Conference on Electrical Machines and Power Electronics, March 14-15*. London, United Kingdom, pp 1072-1078.
- [20] Menoufi K., 2017. Dust accumulation on the surface of photovoltaic panels: Introducing the Photovoltaic Soiling Index (PVSI). *Sustainability*. 9(6).
- [21] Abid A., Obed A., and Al-Naima F., 2018. Detection and control of power loss due to soiling and faults in photovoltaic solar farms via wireless sensor network. *International Journal of Engineering and Technology* 7(2): 718–724.
- [22] Makrides G., Zinsser B., Norton M., and Georghiou G.E., 2012. Performance of photovoltaics under actual operating conditions. Chapter 9, *Third Generation Photovoltaics*, ed. Vasilis Fthenakis, InTech.
- [23] Mani M. and R. Pillai. 2010. Impact of dust on solar photovoltaic (PV) performance: Research status, challenges and recommendations. *Renewable and Sustainable Energy Reviews* 14(9): 3124–3131.
- [24] Maghami M.R., Hizam H., Gomes C., Radzi M.A., Rezadad M.I., and Hajjighorbani S., 2016. Power loss due to soiling on solar panel: A review. *Renewable and Sustainable Energy Reviews* 59: 1307–1316.
- [25] Mejia F.A. and J. Kleissl. 2013. Soiling losses for solar photovoltaic systems in California. *Solar Energy* 95: 357–363.
- [26] Pedersen H., Strauss J., and Selj J., 2016. Effect of soiling on photovoltaic modules in Norway. *Energy Procedia* 92: 585–589.
- [27] Costa S.C.S., Diniz A.S.A.C., and Kazmerski L.L., 2016. Dust and soiling issues and impacts relating to solar energy systems: Literature review update for 2012-2015. *Renewable and Sustainable Energy Reviews* 63: 33–61.

- [28] Chandra S., Agrawal S., and Chauhan D.S., 2018. Effect of ambient temperature and wind speed on performance ratio of polycrystalline solar photovoltaic module: An experimental analysis. *International Energy Journal* 18(2): 171 – 180.
- [29] Said S.A.M., Hassan G., Walwil H.M., and Al-Aqeeli N., 2018. The effect of environmental factors and dust accumulation on photovoltaic modules and dust-accumulation mitigation strategies. *Renewable and Sustainable Energy Reviews* 82: 743–760.
- [30] Banavar M., Braun H., Buddha S.T., Krishnan V., Spanias A., Takada S., Takehara T., Tepedelenlioglu C., and Yeider T., 2012. *Signal Processing for Solar Array Monitoring, Fault Detection, and Optimization*. Synthesis lectures on Power Electronics, September 2012, 7(1): 1-95 Morgan & Claypool Publishers.
- [31] Wurster T.S. and M.B. Schubert. 2014. Mismatch loss in photovoltaic systems. *Solar Energy* 105: 505–511.
- [32] Evans R., Boreland M., and Green M.A., 2018. A holistic review of mismatch loss: From manufacturing decision making to losses in fielded arrays. *Solar Energy Materials and Solar Cells* 174: 214 – 224.
- [33] Mellit A., Tina G.M., and Kalogirou S.A., 2018. Fault detection and diagnosis methods for photovoltaic systems: A review. *Renewable and Sustainable Energy Reviews* 91: 1 – 17.
- [34] Dutta S. and K. Chatterjee. 2018. A buck and boost based grid connected PV inverter maximizing power yield from two PV arrays in mismatched environmental conditions. *IEEE Transactions on Industrial Electronics* 65: 5561 – 5571.
- [35] Mahmoud Y. and E.F. El-Saadany. 2017. Enhanced reconfiguration method for reducing mismatch losses in PV systems. *IEEE Journal of Photovoltaics* 7(6): 1746 – 1754.
- [36] Bayrak F., Ertürk G., and Oztop H.F., 2017. Effects of partial shading on energy and exergy efficiencies for photovoltaic panels. *Journal of Cleaner Production* 164: 58 – 69.
- [37] Paudyal B.R. and S.R. Shakya. 2016. Dust accumulation effects on efficiency of solar PV modules for off grid purpose: A case study of Kathmandu. *Solar Energy* 135: 103–110.
- [38] Al-naima F.M. and A.G. Albaali. 2013. Analysis of dust parameters and evaluation of their impact on solar photovoltaic panel performance. In *Proceedings of International Conference on Renewable Energy and its Future in the Arab World 2013 (ICREFAW)*, Amman, Jordan.
- [39] Moradi M.H. and A.R. Reisi. 2011. A hybrid maximum power point tracking method for photovoltaic systems. *Solar Energy* 85(11): 2965 – 2976.
- [40] Hohm D.P. and M.E. Ropp. 2000. Comparative study of maximum power point tracking algorithms using an experimental, programmable, maximum power point tracking test bed. In *Proceedings of IEEE Photovoltaic Specialists Conference*, September 2001. Arkansas, USA. Conference record of the Twenty-Eight IEEE, pp. 1699–1702.
- [41] Azevedo G.M.S., Cavalcanti M.C., Oliveira K.C., Neves F.A.S., and Lins Z.D., 2008. Evaluation of maximum power point tracking methods for grid connected photovoltaic systems. In the *39th IEEE Annual Power Electronics Specialists Conference (PECS)*, 15-19 June 2008, Rhodes, Greece, pp. 1456–1462.
- [42] Zhao Y., de Palma J., Mosesian J., Lyons R., and Lehman B., 2013. Line-Line fault analysis and protection challenges in solar photovoltaic arrays. *IEEE Transactions on Industrial Electronics* 60(9): 3784 – 3795.
- [43] Albers M.J. and G. Ball. 2015. Comparative evaluation of DC fault-mitigation techniques in large PV systems. *IEEE Journal on Photovoltaics* 5(4): 1169 – 1174.

